

Segmentation of Skin Images using Fixed Grid Wavelet Networks

S. V. Sugin

ME- Computer Science and Engineering, Infant Jesus College of Engineering and Technology.

Mr. A. Jegadeesh

Assistant Professor, Dept of Computer Science and Engineering,
Infant Jesus College of Engineering and Technology.

Abstract: - In this paper, a novel method for the segmentation of skin lesions in Skin images based on wavelet network (WN) is proposed. The WN presented here is a static-grid with no need of training. To enhance the network structure and to estimate the network weights the orthogonal least squares algorithm is used. Here, the network inputs and the network structure formation are considered as the R, G, and B values of Skin image. Then, the image is segmented and the skin lesions accurate boundary is determined. The segmentation algorithm were employed to 30 Skin images and calculated with 11 different metrics, by means of the segmentation result found by a skilled pathologist as the ground truth.

IndexTerms:Image segmentation,orthogonal least squares (OLS), wavelet network (WN).

thresholding on optimal color channels. These methods are so numerous that comparing them and discussing their advantages and disadvantages has taken the full length of many articles.

Artificial intelligence field, especially using fuzzy and artificial neural network (NN) approaches for segmentation of medical images, has gain special popularity. One of the most promising computational intelligence methods that has been widely used for various applications in different areas is wavelet network (WN). The main advantage of WNs over similar architectures such as multilayer perceptron (MLP) and networks of radial basis functions (RBF) is the possibility of optimizing the WN structure by means of efficient deterministic construction algorithms.

I. INTRODUCTION

Among all the types of skin cancer, is the most dangerous and deadly. Fortunately, despite its increasingly spread, it is not an untreatable disease if diagnosed at rudimentary stages. The various features such as color, shape, and texture were extracted. Later on, the more precise and advanced imaging technique, namely skin images, offered a noninvasive method for in vivo observation of pigmented skin lesions used in dermatology. The standard approach in automatic skin image analysis has usually three stages: 1) image segmentation; 2) feature extraction and feature se-lection; and 3) lesion classification. Due to different shapes and colors of skin, segmentation is the most important stage of all.

There have been a great number of algorithms for segmenting skin images, such as fuzzy c means clustering, thresholding, gradient vector flow (GVF), quantitative assessment of tumor extraction, j-image segmentation algorithm, independent histogram pursuit algorithm, k-means++, statistical region merging, dermatologist-like tumor are extraction algorithm, adaptive snake, thresholding based on type-2 fuzzy logic, wavelet transform (WT) fuzzy algorithms, iterative classification, modified random walker algorithm, and hybrid

II.WAVELET NETWORK

1. Structure of WN

The output signal of a WN with one output y , d inputs $\mathbf{x} = (x_1, x_2, \dots, x_d)^T$ and q wavelons (wavelet neurons) in the hidden layer is,

$$y = \sum_{i=1}^q w_i \psi_{m_i, n_i}(\mathbf{x}) = \sum_{i=1}^q w_i 2^{-m_i d/2} \psi(2^{m_i} \mathbf{x} - \mathbf{n}_i)$$

here w_i , $i = 1, 2, \dots, q$, are weight coefficients, ψ_{m_i, n_i} are dilated and translated versions of a mother wavelet function $\psi: \mathbb{R}^d \rightarrow \mathbb{R}$, and m_i , n_i are scale and shift parameters, respectively. NNs are known to suffer from lack of robustness toward outliers. In contrast, due to time-frequency localization of the WT and the self-learning characteristic of NNs, WN is more effective and robust than NN.

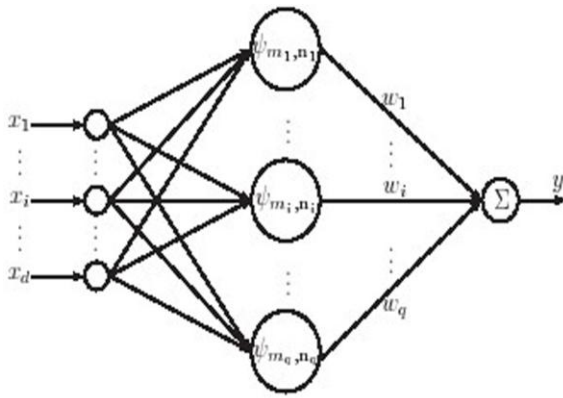


Fig 1: Three-layered WN Structure.

2. Algorithm for Building an FGWN

A major advantage of WNs over other neural architectures is the availability of efficient construction algorithms for defining the network structure. In FGWN, after determining the structure, the weights w_i can be obtained through linear estimation techniques. In this study, a constructive method is employed to build an FGWN. It can be described as follows.

Algorithm 1: Suppose we have M input–output data in the form $\{(x^{(k)}, y^{(k)}), k = 1, 2, \dots, M\}$, where $x^{(k)} = [x^{(k)}_1, \dots, x^{(k)}_d]^T$ is the input d -dimensional vector and inputs matrix is the form $X = [x^{(1)} \dots x^{(k)} \dots x^{(M)}]$. The output vector is considered as $y = [y^{(1)} \dots y^{(k)} \dots y^{(M)}]^T$. The FGWN structure is determined by a ten-stage algorithm.

1) (Normalization): In many cases, input data of WN vary within a wide range and this variability reduces the efficiency of WN. Thus, this first stage is considered as the data preprocessing stage in which the input data are normalized to a certain range in order to avoid data scattering. If for k^{th} input: $T_k = \max_{q=1, \dots, dx} x_q(k)$, $t_k = \min_{q=1, \dots, dx} x_q(k)$, then for mapping the input data to range $[a, b]$, the following equation is used:

$$x_{q, new}^{(k)} = \frac{b - a}{T_k - t_k} x_{q, old}^{(k)} + \frac{aT_k - bt_k}{T_k - t_k}$$

2) (Formation of wavelet lattice): In this step regarding a hyper shape on wavelet parameters space that was selected in the previous stage, the wavelet function is calculated for all the input vectors according to following equation:

$$\psi_{m_i, n_j}(\mathbf{x}) = 2^{-m_i d/2} \psi(2^{m_i} \mathbf{x} - \mathbf{n}_j)$$

The number of nodes in a wavelet lattice is too many; therefore, it is obligatory that the number of these nodes be lowered and the shift and scale parameters of effective wavelets be selected. It is done through two stages of screening as follows.

3) (Primary screening): In this stage, for every scale level selected in stage 4, I_k set is formed for each input vector according to

$$I_k = \{(m, \mathbf{n}) : |\psi_{m_i, n_j}(\mathbf{x})| \geq \epsilon \max_i |\psi_{m_i, n_j}(\mathbf{x})|\}$$

In fact, in this stage, the effective support of wavelets is selected.

4) (Secondary screening): In this stage, the shift and scale parameters of wavelets that are selected in at least two set of the sets in stage 5 are determined. In this way, set I is formed as follows:

$$I = \{(m, \mathbf{n}) : \text{if}[(m, \mathbf{n}) \in I_{k_r}, (m, \mathbf{n}) \in I_{k_l}] \Rightarrow r \neq l\}$$

if the nodes with red circles are assumed as members of set I_{k_r} and nodes with blue circles as members of set I_{k_l} , the nodes with circles in both red and blue colors would be the members of set I .

The fact that screening in this study is performed in two stage is its novel and distinguishing feature which makes the wavelet lattice globalized.

III. SEGMENTATION ALGORITHM

The algorithm from the previous stage is used in the present stage for segmentation of the skin images. From images database, a number of images are randomly chosen for formation of FGWN. At first the values of R, G, and B matrices of each color skin image are mapped into $[0, 1]$ range by performing normalization process.

$$x_{q, new}^{(k)} = \frac{x_{q, old}^{(k)} - t_k}{T_k - t_k}$$

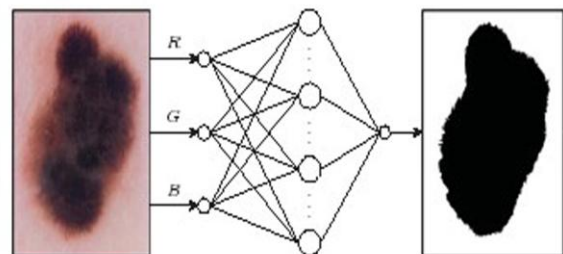


Fig 2: FGWN for Segmentation of Skin Images.

Then, an FGWN is formed with three inputs, a hidden layer, and an output. In order to form the FGWN, the values of three color matrices are considered as network inputs. These matrices are related to the five chosen images from the selected images for segmentation. From these images, some pixels are selected randomly (ranging from 1000 to 5000 pixels for a 485×716 image). If the pixel is

inside the lesion, network output will be considered as 0, and if the pixel is outside the lesion, the output will be considered as 1.

IV. RELATED WORK

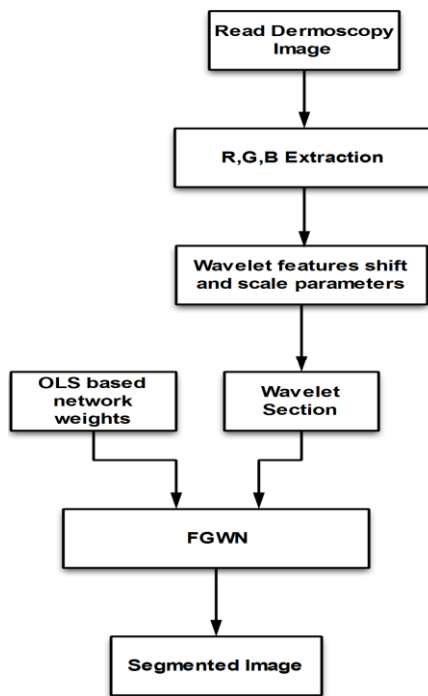


Fig 3: System Structure

1. Preprocessing

In preprocessing, each image will undergo several stages of filtering to remove any unwanted information. The reason why the filtering is needed is because it will reduce the data size of the image and will make the processing time much faster. After all the images are the same size, color extraction means the RGB channel extraction will be done. After color extraction, the input data are normalized to a certain range in order to avoid data scattering.

2. Feature Extraction

To extract information needed from the image, a feature extraction technique will be carried out. The features are extracted using two feature extraction methods which are co-occurrence matrix approach, known as grey level co-occurrence matrix (GLCM) and also Gabor filters to generate more variation of features.

3. Post processing

Since extracting the features of lesion is the most essential part of diagnosing melanoma, extracting the exact boundary of lesion is a vital task. For this, after segmentation with an FGWN and according to the proposed algorithm, the space between two shapes is filled, extra parts are eliminated, and the noise is removed. Then,

the exact boundary of lesion is extracted. This is done by appropriate morphological processes, including erosion, dilation, closing and opening, and region filling. Size, shape, and kind of structuring elements were based on images dimensions and type of their objects that are selected tentatively and provisionally.

4. Orthogonal Least Squares (OLS)

To select the best subset of W , assuming that the size of this subset is known and denoted as s , at first, the most significant wavelets in W is selected. Next, all other (not selected) wavelets are made orthogonal to the selected one. In the second step of the algorithm, the most significant of the remaining wavelets is again selected; then, in this step, all non selected wavelets are made orthogonal with respect to the selected one, so that second selected wavelet with addition to the first one can determine the best approximation. And then, the algorithm goes on for the rest of wavelets. Since all remaining wavelets are made orthogonal to all selected ones in each step of the algorithm, the improvement of each selectable wavelet is isolated.

5. Evaluation of Results

For our test assessment, we utilized a PC with Intel(R) Core (TM) 2 Due CPU T9550 (2.66GHz) and 4 GB RAM. All the methods were realized by MATLAB7.12.

In performance evaluation, the proposed algorithm is compared with the existing algorithm.

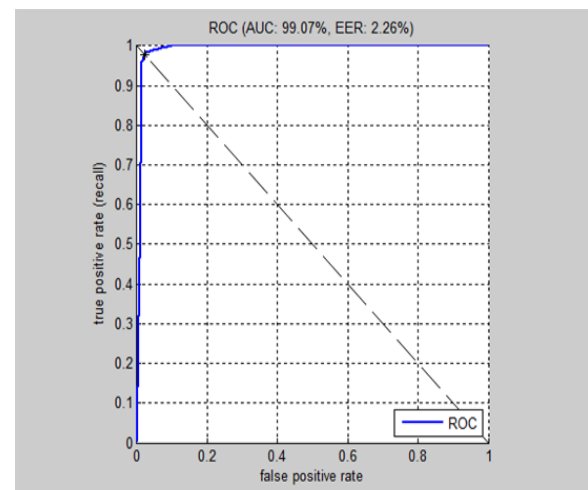


Fig 4: Performance Analysis

V. FUTURE WORK

In the future we apply Fuzzy weighted learning instead of orthogonal least squares (OLS) for improving the segmentation accuracy.

VI.CONCLUSION

In this study, another methodology is proposed for division of skin pictures dependent upon FGWN. The R, G, and B qualities of a skin picture are recognized as FGWN inputs and the OLS calculation is utilized to focus the system weights and to upgrade the system structure. The proposed system with four systems (AT, GVF, FBSM, and NN) and hand division by a pro and dependent upon 11 criteria indicated better brings about correlation to comparative past studies.

REFERENCES

- M. E. Celebi, H. Kingravi, B. Uddin, H. Iyatomi, A. Aslandogan, W. V. Stoecker, and R. H. Moss, "A methodological approach to the classification of dermoscopy images," *Comput. Med. Imag. Graph.*, vol. 31, no. 6, pp. 362–373, Sep. 2007.
- H. Zhou, M. Chen, L. Zou, R. Gass, L. Ferris, L. Drogowski, and J. Rehg, "Spatially constrained segmentation of dermoscopy images," in *Proc. 5th IEEE Int. Symp. Biomed. Imag.: Nano Macro*, May 2008, pp. 800–803.
- M. E. Celebi, H. A. Kingravi, H. Iyatomi, Y. A. Aslandogan, W. V. Stoecker, R. H. Moss, J. M. Malters, J. M. Grichnik, A. A. Marghoob, H. S. Rabinovitz, and S. W. Menzies, "Border detection in dermoscopy images using statistical region merging," *Skin Res. Technol.*, vol. 14, no. 3, pp. 347–353, Aug. 2008.
- S.A. Billings and H.L. Wei, "A new class of wavelet networks for nonlinear system identification," *IEEE Trans. Neural Netw.*, vol. 16, no. 4, pp. 862–874, Jul. 2005.
- A. G. Isasi, B. G. Zapirain, and A. M. Zorrilla, "Melanomas non-invasive diagnosis application based on the ABCD rule and pattern recognition image processing algorithms," *J. Comput. Biol. Med.*, vol. 41, no. 9, pp. 742–755, Sep. 2011.
- T. Buhl, C. H.-Hagge, B. Korpas, K. M. Kaune, E. Haas, A. Rosenberger, M. P. Schon, S. Emmert, and H. A. Haenssle, "Integrating static and dynamic features of melanoma: The DynaMel algorithm," *J. Amer. Acad. Dermatol.*, vol. 66, no. 1, pp. 27–36, Jan. 2012.
- M. Silveria, J. C. Nascimento, J. S. Marques, A. R. S. Marcal, T. Mendonca, S. Yamauchi, J. Maeda, and J. Rozeira, "Comparison of segmentation methods for melanoma diagnosis in dermoscopy images," *IEEE Trans. Signal Process.*, vol. 3, no. 1, pp. 35–45, Mar. 2009.
- P. Schmid, "Segmentation of digitized dermatoscopic images by twodimensional color clustering," *IEEE Trans. Med. Imag.*, vol. 18, no. 2, pp. 164–171, Feb. 1999.
- H. Ganster, P. Pinz, R. Rohrer, E. Wildling, M. Binder, and H. Kittler, "Automated melanoma recognition," *IEEE Trans. Med. Imag.*, vol. 20, no. 3, pp. 233–239, Mar. 2001.
- B. Erkol, R. H. Moss, R. J. Stanley, W. V. Stoecker, and E. Hvatum, "Automatic lesion boundary detection in dermoscopy images using gradient vector flow snakes," *Skin Res. Technol.*, vol. 11, no. 1, pp. 17–26, Feb. 2005.
- H. Zhou, G. Schaefer, M. E. Celebi, F. Lin, and T. Liu, "Gradient vector flow with mean shift for skin lesion segmentation," *Comput. Med. Imag. Graph.*, vol. 35, no. 2, pp. 121–127, Mar. 2011.
- H. Iyatomi, H. Oka, M. Saito, A. Miyake, M. Kimoto, J. Yamagami, S. Kobayashi, A. Tanikawa, M. Hagiwara, K. Ogawa, G. Argenziano, H. P. Soyer, and M. Tanaka, "Quantitative assessment of tumour extraction from dermoscopy images and evaluation of computer-based extraction methods for an automatic melanoma diagnostic system," *Melanoma Res.*, vol. 16, no. 2, pp. 183–190, 2006.
- M. E. Celebi, Y. A. Aslandogan, W. V. Stoecker, H. Iyatomi, H. Oka, and X. Chen, "Unsupervised border detection in dermoscopy images," *Skin Res. Technol.*, vol. 13, no. 4, pp. 454–462, Nov. 2007.
- D. D. Gomez, C. Butakoff, B. K. Ersboll, and W. Stoecker, "Independent histogram pursuit for segmentation of skin lesions," *IEEE Trans. Biomed. Eng.*, vol. 55, no. 1, pp. 157–161, Jan. 2008.
- H. Iyatomi, H. Oka, M. E. Celebi, M. Hashimoto, M. Hagiwara, M. Tanaka, and K. Ogawa, "An improved internet-based melanoma screening system with dermatologist-like tumor area extraction algorithm," *Comput. Med. Imag. Graph.*, vol. 32, no. 7, pp. 566–579, Oct. 2008.
- M. E. Yuksel and M. Borlu, "Accurate segmentation of dermoscopic images by image thresholding based on type-2 fuzzy logic," *IEEE Trans. Fuzzy Syst.*, vol. 17, no. 4, pp. 976–982, Aug. 2009.
- H. Castillejos, V. Ponomaryov, and L. N.-de-Rivera, V. Golikov, "Wavelet transform fuzzy algorithms for dermoscopic image segmentation," *J. Comput. Math. Meth. Med.*, vol. 2012, pp. 41–52, 2012.
- M. Zorzea, S. O. Skrvseth, T. R. Schopf, H. M. Kirchesch, and F. Godtliebsen, "Automatic segmentation of dermoscopic images by iterative classification," *Int. J. Biomed. Imag.*, vol. 2011, p. 19, 2011.
- P. Wighton, M. Sadeghi, T. K. Lee, and M. S. Atkins, "A fully automatic random walker segmentation for skin lesions in a supervised setting," in *Proc. 12th Int. Conf. Med. Imag. Comput. Assist. Int. Part II*, Sep. 2009, pp. 1108–1115.
- R. Garnavi, M. Aldeen, M. E. Celebi, G. Varigos, and S. Finch, "Border detection in dermoscopy images using hybrid thresholding on optimized color channels," *Comput. Med. Imag. Graph.*, vol. 35, no. 2, pp. 105–115, Mar. 2011.
- M. E. Celebi, H. Iyatomi, G. Schaefer, and W. Stoecker, "Lesion border detection in dermoscopy images," *Comput. Med. Imag. Graph.*, vol. 33, no. 2, pp. 148–153, Mar. 2009.
- P. Wighton, T. K. Lee, H. Lui, D. I. McLean, and M. S. Atkins, "Generalizing common tasks in automated skin lesion diagnosis," *IEEE Trans. Inf. Tech. Biomed.*, vol. 15, no. 4, pp. 622–629, Jul. 2011.
- K.-S. Cheng, J.-S. Lin, and C.-W. Mao, "Techniques and comparative analysis of neural network systems and fuzzy systems in medical image segmentation," *Fuzzy Theor. Syst. Tech. Appl.*, vol. 3, pp. 973–1008, 1999.
- J. Jiang, P. Trundle, and J. Ren, "Medical image analysis with artificial neural networks," *Comput. Med. Imag. Graph.*, vol. 34, no. 8, pp. 617–631, Dec. 2010.
- R. M. Balabin, R. Z. Safieva, and E. I. Lomakina, "Wavelet neural network (WNN) approach for calibration model building based on gasoline near infrared (NIR) spectra," *J. Chemometr. Intell. Lab. Syst.*, vol. 93, no. 1, pp. 58–62, Aug. 2008.
- Q. Zhang and A. Benveniste, "Wavelet networks," *IEEE Trans. Neural Netw.*, vol. 3, no. 6, pp. 889–898, Nov. 1992.
- Y. C. Pati and P. S. Krishnaprasad, "Analysis and synthesis of feedforward neural networks using discrete affine wavelet transformations," *IEEE Trans. Neural Netw.*, vol. 4, no. 1, pp. 73–85, Jan. 1992.
- H. H. Szu, B. A. Telfer, and S. L. Kadambe, "Neural network adaptive wavelets for signal representation and classification," *Opt. Eng.*, vol. 31, no. 9, pp. 1907–1916, Sep. 1992.
- H. Zhang, B. Zhang, W. Huang, and Q. Tian, "Gabor wavelet associative memory for face recognition," *IEEE Trans. Neural Netw.*, vol. 16, no. 1, pp. 275–278, Jan. 2005.
- X.-B. Wen, H. Zhang, and F.-Y. Wang, "A wavelet neural network for SAR image segmentation," *J. Sens.*, vol. 9, no. 9, pp. 7509–7515, Sep. 2009.
- A. Abhyankar and S. A. C. Schuckers, "A novel biorthogonal wavelet network system for off-angle iris recognition," *J. Pattern Recognit.*, vol. 43, no. 3, pp. 987–1007, Mar. 2010.
- O. Jemai, M. Zaied, C. B. Amar, and M. A. Alimi, "Pyramidal hybrid approach: Wavelet network with OLS algorithm-based image classification," *Int. J. Wavel. Multir. Inf. Process.*, vol. 9, no. 1, pp. 111–130, Mar. 2011.
- R. Galvao, V. M. Becerra, and M. F. Calado, "Linear-wavelet networks," *Int. J. Appl. Math. Comput. Sci.*, vol. 14, no. 2, pp. 221–232, Aug. 2004.
- Q. H. Zhang, "Using wavelet network in non parametric estimation," *IEEE Trans. Neural Netw.*, vol. 8, no. 2, pp. 227–236, Mar. 1997.
- J. Gonzalez-Nuevo, F. Argueso, M. Lopez-Caniego, L. Toffolatti, J. L. Sanz, P. Vielva, and D. Herranz, "The Mexican hat wavelet family application to point source detection in CMB maps," *Mon. Not. Roy. Astron. Soc.*, vol. 369, pp. 1603–1610, 2006.